PHENIX Muon Identifier

H. Akikawa [f] T. Awes [i] F. Bellaiche [i,1] M. Bobrek [i] T.V. Cianciolo [i]
Y. Efremenko [n,i] H. En'yo [j,f] E. Fujisawa [m] H. Funahashi [f] T. Gee [i]
A. Glenn [n] G. Gogiberidze [n] N. Hayashi [j,2] S. Held [i,3] S. Hicks [i]
J. Hill [d] D. Hurst [i] T. Ichihara [j,k] K. Imai [f] M. Ishihara [j,k]
J. Johnson [i] Y. Kamyshkov [n,i] L. Kotchenda [l] K. Kurita [j]
J. Lajoie [d] Z. Li [j,b] X. Liu [a,b] Y. Mao [j,b] S. Mioduszewski [n,4]
J. Nagle [c] Y. Nakada [f] J. Newby [n] F. Obenshain [i] F. Plasil [i]
K. Pope [n] G. Rao [i] K. Read [i,n] R. Roth [g,5] N. Saito [j,k] T. Sakuma [m]
H.D. Sato [f] M. Sekimoto [e] T. Shibata [m] H. Skank [d] D. Smith [i]
S. Sorensen [n,i] P. Stankus [i] S. Steffens [n] E. Stein [a] W. Stokes [a]
Z. Sun [b] A. Taketani [j] E. Taniguchi [m] J. Tojo [f] H. Torii [f]
W. Tian [i,b,6] J. Tradeski [a] Y. Wan [b] Y. Watanabe [j,k] L. Watkins [i]
R. Whitus [i] C. Williams [i] Y. Yang [a,b] S. Yoneyama [m] G. Young [i]
S. Zhou [b]

[a] *Brookhaven National Laboratory, Upton, NY 11973*

[b] *China Insitute of Atomic Energy (CIAE), Beijing, People's Republic of China*

[c] *Columbia University, New York, New York 10027*

[d] *Iowa State University, Ames, Iowa 50011*

[e] *KEK, High Energy Research Accelerator Organization, Tsukuba-shi, Ibaraki-ken 305-0801, Japan*

[f] *Kyoto University, Kyoto 606, Japan*

[g] *Los Alamos National Laboratory, Los Alamos, New Mexico 87545*

[h] *Nevis Laboratories, Irvington, New York 10533*

[i] *Oak Ridge National Laboratory, Oak Ridge, Tennessee 37831*

[j] *RIKEN (The Institute of Physical and Chemical Research), Waco, Saitama 351-0198, Japan*

[k] *RIKEN BNL Research Center, Brookhaven National Laboratory, Upton, NY 11973*

[l] *State Interphysica, Protvino, Russia*

[m] *Department of Physics, Tokyo Institute of Technology, Tokyo, 152-8551, Japan*

[n] *University of Tennessee, Knoxville, TN 37996*

In this paper we describe the PHENIX Muon Identifier.

1 Introduction

The irreducible μ/π ratio due to weak decay is approximately 1×10^{-3} (primarily determined by the proximity of the nosecone to the vertex). We set a detector design criteria to 1/4 of this, namely 2.5×10^{-4}, for a pion from the vertex to be misidentified as a muon (forming part of a dimuon). The factor of 1/4 provides over an order of magnitude suppression for the *pair* background. Thus, the irreducible background of muons reaching the muon identifier, as opposed to the muon identifier design and the algorithms used to reject the larger hadron background, will set the ultimate physics background level. Of this required net μ/π separation, approximately 10^{-2} is provided by the presence of the absorber preceding the muon identifier which filters out pions. This leaves 3% as the maximum tolerable fraction of the charged pions which may subsequently be misidentified as muons.

The punchthrough probability versus depth of steel for muons of various momenta are plotted in [**?**] and [**?**]. In order to set the punchthrough probability for muons of up to 4 GeV/c to be 3% or less, a total steel depth of 90 cm (5.4 hadronic interaction lengths) is required beyond the nosecone and central magnet. Subtracting the thickness of the muon magnet backplate, a total depth of 60 cm of steel is required in the muon identifier itself.

A muon at the vertex must have a mean energy of at least 1.9 GeV to reach the muon identifier system. The mean minimum original energy to penetrate completely through the muon identifier is 2.7 GeV [**?**].

2 Detector Design

Ideally, the 60 cm of steel is to be distributed in a sandwich interleaved with detector layers. The detectors themselves require a non-negligible amount of space and the total available space in z is quite limited in the PHENIX detector hall (2.7 m). Also, it is desirable to have the early absorber layers be divided more finely to increase the acceptance for ϕ meson detection. Segmentation also improves the measurement of the trajectory in the identifier. The segmentation chosen is a total of four steel absorbers after the 30 cm thick muon magnet backplate of the north arm of thicknesses 10, 10, 20, 20 cm. The 5 gaps created by the absorbers are instrumented with the muon identifier panels. The muon identifier for the south arm is identical to that for the north arm (although the muon magnet backplate is only 20 cm thick) and at the same distance from the interaction vertex. Maintaining the

[1] Present address: Bellaiche's French Institute
[2] Present address: JAERI, Japan
[3] Present address: Knoxville High School, Knoxville, Tennessee 379xx
[4] Present address: Brookhaven National Laboratory, Upton, NY 11973
[5] Present address: Columbia University, New York, New York 10027
[6] Present address: University of Tennessee, Knoxville, TN 37996

same design for both arms helped minimize design costs.

Beam gas studies show that for low polar angles (20° or less), an effective segmentation into logical pads of approximately 13 by 13 cm is required to suppress false roads for tracks in the muon identifier. Rather than develop Iarocci tubes of greater width or use 13 cm wide external strips, the most cost effective solution is simply to use standard Iarocci tubes of width 8.5 cm with all eight internal wires ganged together. This provides a readout pitch of 8.5 cm along both the x and y directions, thus providing effective 8.5 cm square hodoscopic cells (upon forming the appropriate ANDs). This most cost effective solution exceeds our requirements. This segmentation is fine enough to provide sufficient granularity for matching roads in the identifier to tracks in the muon tracker unambiguously with anticipated occupancies.

We use the term Iarocci tubes to refer to planar drift tubes consisting of 100-μm gold-coated CuBe anode wires at the center of long channels of a graphite-coated plastic cathode, with a gas mixture such as Isobutane-CO_2. This same physical detector when operated at higher voltage is a conventional limited streamer tube [**?**]. We operate them in the proportional mode to increase longevity. They are proportional tubes operated at a voltage such that only a fraction of the signals are not proportional mode pulses.

We apply 4500 V to the anode wires. Incident minimum ionizing particles ionize the gas and create an avalanche. Using a high voltage decoupling capacitor, we read out the signal on the anode wire. The drift time interval (for arrival of 90% of pulses) in the tube is approximately 100 ns for a 9:91 Isobutane-CO_2 gas mixture.

A	B	C
D	E	F

Table 1
Panel arrangement viewed from origin.

Iarocci tubes were chosen because they satisfy all of the detector performance criteria discussed above. They have proven reliability and longevity, compactness, low cost, and are readily available from commercial vendors [**?**]. Such tubes can be used economically to tile large areas. They have robust wires and seals. They avoid the problems of metal-plastic transitions present at the endcaps for aluminum proportional tubes.

Tubes with 9 mm by 9 mm channels satisfy the count-rate and position localization requirements, but must be staggered by half a cell and ORed in pairs (discussed below) and/or operated with a fast gas (discussed below) to meet the timing requirements of the Local Level 1 (LVL-1) trigger system.

An individual anode wire and the immediately surrounding gas volume and graphite-coated walls are referred to as one channel of an Iarocci

Panels	Horizontal	Length	Vertical	Length
A,C,D,F	118H	5200 mm	128V	5010 mm
B,E	90H	2504 mm	52V	3821 mm

Table 2
Number and lengths of Iarocci tubes per panel.

Quantity	Value
panels/gap	6
panels/arm	30
tubes/gap	1268
tubes/arm	6340
area/gap	13.1 m × 10.7 m

Table 3
Muon identifier specifications.

tube. Each wire is held at the center of its channel by means of plastic wire spacers positioned every 50 cm along the tube.

The term Iarocci tube refers to the ready-to-go detector element consisting of eight channels. Its principal components are the comb profile, the wire, wire spacers, outer jacket, and plastic endcaps. A two-pack is a pair of tubes connected together and staggered by half a channel. Their signals are OR'd together. Groups of two-packs oriented both horizontally and vertically are held inside an aluminum box. Approximately half are oriented horizontally and half are oriented vertically so that both projections are measured. This total detector element is called a muon identifier panel. There are six such panels per gap labelled A through F as shown in Table 1.

The number and lengths of tubes inside every panel are listed in Table 2. Overall specifications are listed in Table 3. Adjacent panels overlap along their edges to eliminate the creation of any deadspace by the panel frames. The panel frames are shown in Figure **??**. Panels (A, C, and E) lie in one plane which is 10 cm closer to the vertex than the plane of the other panels (B, D, and F).

The muon identifier has panels hanging in two parallel rails attached to the MuID steel in a given gap. Figure **??** shows panels A,C and E, all of which hang in a single rail. The lower panel E hangs from two rods which are secured to the rail just to the inside of panels A and C. The connection points for gas and electrical services are shown, as are the optical survey targets.

Panels B, D and F all hang in a single rail. The lower panels each hang from six rods which are secured to the rail. The connection points for gas and electrical services are shown, as are the optical survey targets.

The acceptance reaches down to 10° in the first plane (and even farther in subsequent planes) except immediately at the four corners of the square beam hole. The elevation view of the north muon arm is shown in Figure **??**.

The tubes are assembled off-site by a commercial vendor and shipped to

our assembly factories located BNL and KEK after having satisfactorily passed quality assurance tests for both gas leakage and high voltage. The tubes are installed into panels at our factories. The assembled and tested muon identifier panels manufactured at BNL will be transported by truck a short distance to the Main Facility Hall. Those assembled in Japan are shipped by cargo ship to BNL. Each will be attached to a special exterior handling frame that can be hoisted using the hall crane. The panels will be inserted in appropriate sequence onto the rails of each gap in order to achieve the desired arrangement. The shield wall ultimately prevent removal of panels.

We require a drift time interval shorter than the time between beam collisions (106 ns) in order to avoid dead time. Shorter drift times reduce the backgrounds associated with the arrival of out-of-time hits such as upstream beam gas events as well as relaxing constraints on the electronics that feeds the LVL-1 trigger system (by providing margin for variations among tubes, cable delay variation, open/closing of latch, drift from cell edge, and time-of-flight from vertex).

The muon identification system has much less stringent alignment to the vertex requirements than the muon tracker since the typical pointing resolution of the system is measured in centimeters and the muon identifier's main function is to work with the muon tracking system. However, since the muon identification system is used in the trigger to find roads which point back to the vertex, there must be some relative alignment of the identifier panels with the interaction point.

The multiple scattering in the absorber material in front of the muon tracking stations limits the angular resolution of a 10 GeV/c track at the vertex to approximately 3 mrad or more. If this error is projected from the first tracking station to the muon identifier, the position resolution is approximately (5.4 m) $\times$ (3×10^{-3}) = 1.6 cm. An additional 1 to 2 mm or error occurs at each of the absorber layers in the muon identifier. Therefore, the muon identifier planes need not be surveyed with respect to the vertex to better than approximately ± 4 mm in the x and y directions in order to have alignment errors be negligible compared to multiple scattering errors. It is only required that the z positions be measured after they are installed, and this measurement only has to be known to within a few centimeters relative to the vertex.

The effective logical pad sizes represented by the transverse tubes of the muon identifier system are 8.5 cm by 8.5 cm. The position resolution along a muon identifier road cannot be expected to be much better than $8.5/\sqrt{12} = 2.5$ cm. If several measurements of resolution 2.5 cm are used, then a projection error of somewhat less than 2.5 cm might be expected. Multiple scattering due to the 30 cm thick muon magnet backplate causes a projection error of 2 mm for a 10 GeV/c track in the tracker to the beginning of a road in the first plane of the muon identifier.

We require alignment of the muon identifier planes with station 3 of the tracking system to ± 1 cm in the x and y directions.

The internal alignment requirements of the muon identification system are determined by its ability to form roads when the tubes are misaligned by a given amount. The individual tubes are 8.5 cm wide. We require alignment errors to be a negligible contribution to the projection error of a road from one plane to the subsequent planes in the identifier system. We require a 5 mm panel to panel alignment in order for road finding in the muon identifier to be limited by multiple scattering. Within a four-pack, we require and can easily achieve a stagger by half a channel to within 1 mm.

The tubes are installed and surveyed within each panel relative to external fiducial marks on each panel to within an accuracy of 2 mm. The external fiducials of the panels can be viewed by conventional survey theodolites located along the west or east sides of the respective arm and down the the main square hole which contains the beam pipe. Using standard survey techniques it is straightforward to measure the absolute positions of the muon identifier detectors to within 3 mm or less which often exceeds our requirements. Panel positions can be adjusted by sliding transversely and by means of lowering rods; however, in most instances we just need to *know* the as-built as-installed positions. Further details concerning muon identifier alignment criteria are discussed in [**?**].

We will record calibration data to obtain samples of cosmic muons, samples of beam gas muons, pedestals, to set discriminator thresholds, monitor timing alignment, monitor HV stabilization, and monitor efficiencies.

We are interested in the efficiency of the two-packs within a timing window of 81 ns (where 81 ns represents the 106 ns between collisions reduced by 25 ns for flip-flop settling and 10 ns for signal transit variation along the length of a tube). Figure **??** shows that at 81 ns, the two-packs are measured to have only a 5% inefficiency when operated with a 9:91 mixture of Isobutane and CO_2.

The MuID has two separate gas volumes. One is primary chamber volume and other is secondary volume, which is the aluminum enclosure of each panel surrounding the primary volume. CO2 and i-C4H10 mixture up to 25feed to the primary volume for chamber operation. N2 is feed to the secondary volume in order to maintain the chamber electronics dry and clean, and diluting the flammable gas component in the case of primary volume leak. The total number of gas circuits is 600 for primary volume and total volume is 50 m**3. The total volume of secondary is 40 m**3. The gas flow rate of primary volume is one volume exchange per day. The gas supply system can recircurate up to 50

3 Readout

We will operate the LSTs in proportional mode to ensure maximum longevity. To ensure adequate signal-to-noise performance in the unknown noise environment at RHIC we settled on a readout scheme that employs in-panel amplification (x150) driving differential signals on 30m twisted-pair cables to a crate-based processing system. Here the signals must be digitized and synchronized such that all signals from a beam crossing arrive simultaneously (a significant challenge given the inherent differences in drift-time, transmission time down the 5m LSTs and large slew for near-threshold hits). Data from every crossing is sent as the Muon arm input to the LVL1 trigger. Trigger latency (for all beam crossings) and readback latency (for LVL1-accepted crossings), required to satisfy the PHENIX pipelined/deadtime-less specification, is provided locally.

The anodes from two half-cell staggered LSTs are capacitively coupled into the amplifier circuit, thus comprising a readout channel. In addition to signal amplification the in-panel portion of the electronics must distribute high voltage to the LSTs. Six readout channels mounted on a $8.2 \times 50.4\,\mathrm{cm}^2$ printed circuit board. Different channels share power buses, a pulser circuit and HV buses. The amplification circuit and HV distribution circuit are mounted on opposite sides of the board so that the HV can be isolated from human contact. The boards are mounted inside the panels at the LST endcaps. The primary requirement for the in-panel portion of the electronics was longevity.

The amplification circuit was based on an L3 design [] with several features incorporated to improve longevity: 1) Resettable polyfuses on the power inputs of each channel, 2) A double-diode protection circuit that allows an amplifier channel to survive even after one of its input LSTs has broken a wire, and 3) Diode clamps to prevent reverse-bias damage. Furthermore, the HV input for each LST has a $400\,\mathrm{M}\Omega$ current-limiting resistor so that the HV for the circuit will continue to operate with multiple tube failures and all HV components are encapsulated in a silicone conformal coating to enhance longevity and safety.

In addition to these steps, we have maintained a design in which different LST planes are on independent separate gas and HV circuits and each plane is further segregated into roughly 24-channel HV, gas and power segments.

The out-panel (post-amplifier) electronics are housed in a set of four 9U crates, each of which has five types of cards described below.

Signals enter the TCs from the back on six 17-pair twisted cables. They are brought into the ROCs through a backplane that simply consists of passthrough pins. This arrangement eases maintenance by allowing the insertion/removal of a ROC without removing the signal cables. The TCs also provide a form-factor transition

from 9U to 6U to allow space for the ROC/FEM communication bus.

The FEM cards are analagous to a conventional crate controller, providing the interfaces between the MUID and the PHENIX online systems (with the exception of LVL1). The ARCNet interface receives the serial control commands, translates them into lower-level instructions that are routed by geographical addressing on the backplane and CPLDs on each card and allows readback of the programmed state. The timing and control interface receives mode bit information and uses a state machine to parse the instructions, validate them and route them to the appropriate places. Upon receipt of a LVL1-accept signal the DCM interface assembles and ships out the data from each ROC in the crate.

One 3U backplane in each crate provides power and digital communication between the ROCs and the FEM. This backplane is modeled after the VME64X backplane (geographical addressing, 10 MHz communication, termination) but has been customized to optimize pin placement and analog power/ground referencing.

The ROCs consist of analog processing and synchronization, buffering, supplemental diagnostics, and serial control.

The first stage of the analog processing chain is a differential receiver for the input signals which converts the signals to single-ended and amplifies them by 3. The signals then go through a novel delay-less constant-fraction discriminator [] to eliminate small-signal slew. Synchronization is obtained in stages through a series of programmable delays and multiplexers that allow the operator to select the optimal clock phase for each channel (by delaying the clock and not the channel we can exchange delay lines for multiplexers, greatly reducing the cost of the system). With this scheme we can synchronize all channels if the following two restrictions are met: 1) all signals coming into a ROC must arrive within one RHIC cycle (106 ns), and 2) the earliest signals into all ROCs must arrive within one RHIC cycle.

The 96 bits of data from each ROC are multiplexed into six 16-bit words and immediately sent via optical G-link to the LVL1 trigger where a steerable road algorithm is implemented to determine if there are candidate muon tracks in the event.

LVL1-trigger latency buffering of 4μs and readback latency buffering for five LVL1-accepted events is provided locally to each ROC. The former is implemented with three 32-bit 64-deep FIFOs (actual depth programable) and the latter is implemented as one FPGA-resident 112-bit 5-deep FIFO. The 112 bits stored for each event include the 96 data bits for that ROC plus a 16-bit beam counter which serves as a timestamp to identify communication errors.

The supplemental diagnostics provide a pulser with 4-channel granularity and individual channel masks. Together these allow for diagnostic

tests of the board itself and to strobe test bit-patterns through the system. In addition, spy lines for both analog signals (immediately after the receiver) and digital signals (after the variable delay) are sent through 96-to-1 serially-controlled multiplexers which drive front-panel LEMO connectors.

The FEM/ROC serial control communication protocol contains an address word that specifies broadcast mode or the geographical address of the ROC being addressed. A second address word specifies the type of data being communicated, e.g., threshold DAC values, programmable delays, etc. Identical CPLDs on each ROC interpret the address and commands and direct the following serial data appropriately.

4 Level-1 Trigger

The mean occupancy in the muon identifier in gap 3 is only 1 hit per event for UA1 events (simulated central collisions without primary muons). Beam gas would be a more serious background (see below); however, we anticipate suppressing this background with shielding. We have developed a trigger algorithm which is very efficient for dimuons, yet has good background rejection. See Ref. [**?**] and [**?**] for a more detailed discussion of the trigger algorithm.

An acceptable dimuon Local Level 1 (LVL-1) trigger for Au-Au running requires the presence of both two or more steered roads as seen in the x-view and two or more steered roads as seen in the y-view. A valid view requires all three of the first three planes to have a hit. Each view points to the origin. In plane 1 it consists of a pair of staggered tubes. For beam gas rejection, we further reject views which are completely parallel to the beam line (and more than 100 cm from the beam line to maintain signal efficiency). We do not choose to phrase the LVL-1 algorithm in terms of $x-y$ intersections in order to minimize the number of possible LVL-1 trigger roads. (There are on the order of 10^4 $x-y$ intersections in a muon identifier plane.) Different running conditions (such as pp collisions for spin physics) will have different backgrounds and will employ somewhat different trigger requirements using the same electronics.

Simulations have shown that the estimated occupancies are low enough in the muon identifier that the ambiguities associated with hodoscopic readout of a panel will not lead to an intolerable LVL-1 trigger rate. Moreover, such ambiguous $x-y$ intersections are immediately resoloved upon matching with tracks in the muon tracker at LVL-2 and offline. These studies were used to justify using hodoscopic readout rather than external pads in order to avoid the costs associated with pad design, development, and fabrication. (The detectors are also thinner without pads and their associated connectors.)

For approximately 80% of J/ψ mesons, both muons penetrate to at least plane 3. Of these, 97.4% will

satisfy the LVL-1 trigger algorithm described above. This rises to near 100% if the straight-view (beam-gas) rejection criterion is removed from the trigger algorithm.

The LVL-1 trigger efficiency is flat as a function of rapidity over almost the entire acceptance.

If not handled properly, beam gas is a potentially very serious background for the muon identifer LVL-1 trigger due to the large number of particles which can enter the detector [**?**]. We expect that specialized absorber shields located in the RHIC tunnel will be required to suppress this background. (See Ref. [**?**] and [**?**] for more details on how we have attempted to estimate this background including development of a new simulated beam gas event generator.) We have estimated that the raw beam-gas event rate is 16 kHz, which is to be compared to the 2 kHz rate of central Au-Au collisions. The design of the LVL-1 trigger plus shielding in the RHIC beam tunnel will be needed in order to keep this background trigger rate under control.

Note that this beam gas event background is mainly a concern for avoiding deadtime associated with the LVL-1 trigger. The background is strongly suppressed at LVL-2 and offline by matching to tracks in the muon tracker and requiring that the track come from within 40 cm of the interaction vertex. This is because tracks in beam gas events are typically parallel to the beam pipe.

Approximately 20% of UA1 events satisfy the LVL-1 trigger algorithm. Thus, the false LVL-1 trigger rate due to central collisions (and neglecting beam gas) is 20% of 2 kHz. This is an acceptable contribution to the total LVL-1 bandwidth and will not introduce dead time. Moreover, this background will be almost completely suppressed by LVL-2. We estimate that the occupancies in the identifier will be entirely tractable providing that the beam gas background is properly shielded.

In order to study the offline performance of the muon identifier, we use a parametrized Monte Carlo simulation of the tracking chamber performance [**?**]. We then match muon identifier roads to the smeared generated tracks in the tracker. Simulations indicate that the matching efficiency is 97%. We then subsequently require that the measured momentum be consistent with the depth penetration in the muon identifier for a muon. Our simulations impose a requirement which is 95% efficient for real muons.

Ultimately, the performance of the muon identifier should be capable of providing an overall μ/π separation ratio of approximately 10^{-4} in order to insure that the dominant backgrounds arise from pion and kaon decay in flight (instead of detector performance). That performance can be obtained after the LVL-2 trigger (or offline) by means of imposing four requirements: (1) the muon identifier road must match to a track in the tracker, (2) the track in the tracker must extrapolate to within

40 cm of the vertex in the transverse plane, (3) the muon road must have a correct depth-momentum relation, and (4) the invariant mass of the reconstructed dimuon must exceed 1 GeV/c^2. We have also studied using multivariate discriminant analysis techniques [**?**] [**?**] in order to investigate possible further improvements in μ/π separation offline.

5 Detector Performance

The drift time interval for conventional 9 mm by 9 mm LSTs with a standard gas (Ar-isobutane) is approximately 100 ns which is too long for our application because it is of the same order as the RHIC bunch crossing time (106 ns). (The rise time and pulse duration are satisfactory, however.) We studied and achieved faster timing characteristics by OR-ing pairs of tubes in a two-pack staggered by half a channel. We thus are able to construct a viable muon identifier using a conventional gas. Note that an important additional reason for the stagger is that it reduces the geometrical inefficiency due to the comb profile septa from 10% to near zero (at normal incidence).

We investigated two other means of obtaining shorter drift times by using faster gas mixtures including CF_4 and by developing Iarocci tubes with a 5 mm by 5 mm cross section, instead of the standard 9 mm by 9 mm as discussed in [**?**].

We have been developing and testing offline software to reconstruct muon events for the PHENIX muon identifier. Single-muon events were simulated and reconstructed to check the reconstruction efficiency of the muon identifer; single-pion events were simulated to see the hadron rejection capability as well. The performance of the muon identifier in high multiplicity was also investigated by mixing J/Ψ signal events with central Au-Au background events.

Table 1. The performance of the muon identifier

Momentum GeV/c	Overall Muon Efficiency (%)	Pion Rejection Rate (%)
2.0	65.3± 1.1	$(2.0 \pm 1.4) \times 10^{-4}$
3.0	93.7± 1.4	$(2.3 \pm 0.5) \times 10^{-3}$
4.0	96.9± 1.4	$(2.5 \pm 0.5) \times 10^{-3}$
5.0	98.1± 1.4	$(3.7 \pm 0.6) \times 10^{-3}$
10.0	99.6± 1.4	$(3.9 \pm 0.7) \times 10^{-3}$

The results had , as shown in Table 1, an overall muon remain rate of about 65-99% in 2.0–10.0GeV/c momentum region, and a pion rejection rate of about 2.0×10^{-4} – 3.9×10^{-3} in the same momentum region. The lower efficiency at 2.0GeV/c is due to the energy loss caused by central magnet and muon identifier absorber. The pion rejection rate is close to the pion decay probability, especially for momentum below 5.0GeV/c. The numbers in Table 1 are consistent to the result from our test experiment in KEK with 1.5-4.0GeV/c pion/muon beam.

In last summer, the PHENIX muon identifier was partially instrumented and operated with pure CO2. The good agreement between number of charged particles in BBC and hit

multiplicity in muon identifier indicates that the real gold-gold collision has been seen by the muon identifier. Figure 1 shows a reconstructed track which points to the collision point.

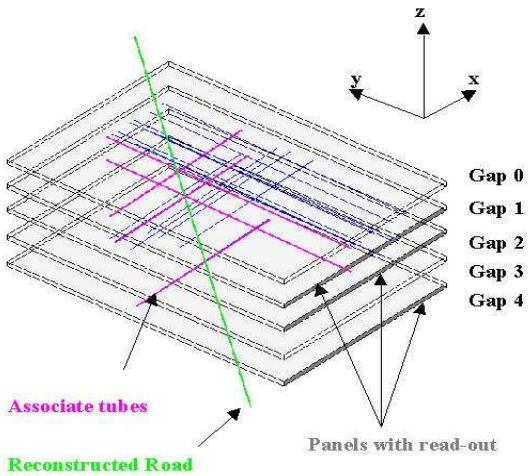

Figure 1

Acknowledgements

We gratefully acknowledge the efforts of the RHIC staff. This work was supported by grants from the U.S. Department of Energy's Nuclear Physics Division.

References

[1] Phys. Rev. C,

[2] Phys. Rev. D.